Catalysis Today 158 (2010) 515–520

Contents lists available at ScienceDirect

Catalysis Today

journal homepage: www.elsevier.com/locate/cattod

Adsorption of simple aromatics from aqueous solutions on modified activated carbon fibers☆

Bingzheng Li[a,b,*], Zhiping Lei[c], Xiaohang Zhang[a], Zhanggen Huang[a,**]

[a] State Key Laboratory of Coal Conversion, Institute of Coal Chemistry, Chinese Academy of Sciences, Taiyuan 030001, PR China
[b] School of Environment & Safety, Taiyuan University of Science and Technology, Waliu Road 66, Taiyuan, Shanxi Province 030024, PR China
[c] School of Chemistry & Chemical Engineering, Anhui University of Technology, Maanshan 243002, PR China

ARTICLE INFO

Article history:
Available online 20 September 2010

Keywords:
ACF
Modification
Aromatics
Adsorption
Surface acidic groups

ABSTRACT

The effects of modification by HNO_3 oxidization on the physico-chemical properties of activated carbon fiber (ACF), the adsorption of aniline, pyridine and phenol on ACF and modified ACF, as well as the influence of textural properties on adsorption by comparing ACF with an activated carbon are investigated. The adsorbents are characterized using N_2 adsorption, Boehm titration, diffuse reflectance infrared Fourier transform spectroscopy, and temperature-programmed desorption. The pore properties of ACF are not significantly changed by the modification; however, it increases greatly the oxygenated acidic groups on the surface of ACF. The uptake for each aromatic compound by the modified ACF is lower than on ACF. This is mainly due to the decrease of dispersive interaction, more water cluster formed to block entry of compounds into micropores or competition between water and compounds adsorbed onto the surface of ACF because of hydrophilic increase of ACF. The maximum uptake for the aromatic compounds decreases with the increase in aqueous solubility of the adsorbates. *K*, a Langmuir parameter, is indirectly associated with the surface chemistry of ACF. For the aromatic compounds mentioned, the uptake increases with the micropore volume of carbon materials.

1. Introduction

Various organic compounds, especially aromatic compounds, can be found in wastewater from chemical industries [1–3]. Due to their flammability, toxicity and carcinogenic properties, many techniques, including biodegradation, sorption, catalytic wet air oxidation, and adsorption–catalytic dry oxidation [4–8], have been studied to remove these compounds from wastewater. Of these, coupling of organic pollutants adsorption in wastewater and catalytic dry oxidation of the adsorbed pollutants over a sorbent-catalyst is a very promising technique for the treatment of dilute wastewater streams containing highly toxic or biorefractory organic pollutants [9–13]. The excellent adsorption capacity of sorbent-catalyst is mainly from their support; therefore, investigating the adsorption behavior of the support is necessary. Among the various adsorptive materials, adsorption by activated carbon (AC) has been mainly used, especially for water and wastewater with low pollutant concentrations [6–8]. AC has an excellent capacity for adsorbing organic compounds, owing to its huge surface area and developed pore characteristics, as well as its surface chemical properties such as the presence of various types of organic groups on the surface [14,15]. The surface chemistry of AC has an effect on its catalytic characteristics, acid–base properties, and adsorption capacity [16]. Occasionally, the surface chemistry is the most important factor in the adsorption process. Activated carbon fiber (ACF), a novel carbon material, is widely recognized as a promising material for removing and preventing pollutants. However, systematic investigation of the influence of modification on the textural and surface chemistry of ACF and the relationship between its surface properties and the adsorption capacity for aromatics is inadequate.

In this study, the influence of texture and surface chemistry of the activated carbon materials on the isothermal adsorption of three aromatic compounds (aniline, phenol, and pyridine) was studied. ACF and AC, with different textural characteristics were selected to investigate the influence of the textural properties. To understand the effect of surface chemistry of the adsorbents, ACF was modified using nitric acid, producing adsorbents that differed mainly in surface chemistry.

☆ This work was presented at the 7th Asia-Pacific Conference on Sustainable Energy and Environmental Technologies (7th APCSEET) held at Qingdao, Shandong, China, October 15–18, 2009.

* Corresponding author at: School of Environment & Safety, Taiyuan University of Science and Technology, Waliu Road 66, Taiyuan, Shanxi Province 030024, PR China. Tel.: +86 351 6962589.
** Corresponding author.
E-mail addresses: lbzh2001@163.com (B. Li), zghuang@sxicc.ac.cn (Z. Huang).

0920-5861/$ – see front matter © 2010 Elsevier B.V. All rights reserved.
doi:10.1016/j.cattod.2010.08.014

2. Experimental

2.1. Adsorbates

The adsorbates studied in this work were aniline, pyridine, and phenol. The aromatics were of analytical grade and dissolved separately in distilled water to yield adsorptive solutions with various concentrations.

2.2. Adsorbents

AC and ACF, used as the control adsorbents, were commercial, coal-based granular activated carbon from Xinhua Chemical Plant (Taiyuan, China) and novel cellulose activated carbon fiber from Shanxi Institute of Coal Chemistry (Taiyuan, China), respectively. AC was crushed into particles of 40–60 mesh size (0.3–0.45 mm) and the ACF was cut into pieces (40 mm × 40 mm); both were finally dried at 110 °C for 48 h.

To obtain adsorbents with similar textural properties and different surface chemistry, the chemical treatment of ACF by HNO_3 oxidation was carried out in a 500 mL Teflon bottle containing 16 g ACF and 200 mL 5 M nitric acid solution at 70 °C for 6 h. Once the oxidation was complete, the oxidized ACF was repeatedly filtered and washed with distilled water several times to remove the impurities. The resulting oxidized ACF was dried at 110 °C for 48 h. The resulting ACF was designated as ACFN.

2.3. Characterization of the adsorbents

2.3.1. Chemical composition

Carbon (C), hydrogen (H), and nitrogen (N) contents of the adsorbents were determined by an element analyzer (Elementar Analysensysteme Gmbh Vario EL), sulfur (S) content was measured by a sulfur analyzer (SC-132, LECO, USA), and oxygen (O) content was calculated by difference.

2.3.2. Texture

The pore structure characteristics of the adsorbents were determined by the N_2 adsorption at 77 K using an automatic ASAP 2020 volumetric sorption analyzer (Micromeritics). The specific surface area (S_{BET}) was calculated using the Brunauer–Emmett–Teller (BET) equation. Micropore volumes of the adsorbents were calculated by *t*-plot. The pore size distribution of the adsorbents was obtained using the density functional theory.

2.3.3. Surface chemistry characterization

There are various techniques for surface chemistry characterization of the activated carbon, including Boehm titration [17,18], Fourier Transform Infrared (FTIR) [16,19], temperature-programmed desorption (TPD) [20,21], and the point of zero charge (pH_{pzc}). Boehm titration is used to quantitatively and qualitatively determine the surface functional groups on the activated carbon. However, some oxygenated functional groups, such as anhydrides and nitrogen-containing groups, cannot be detected by Boehm titration; therefore, diffuse reflectance infrared Fourier transform spectroscopy (DRIFTS) and TPD were used to complement the results from Boehm titration.

2.3.3.1. Boehm titration. An exact amount of adsorbent (0.200 g) was placed in a series of 100 mL well-sealed Teflon bottles containing 25 mL of 0.1 M: NaOH, Na_2CO_3, $NaHCO_3$, and HCl solutions. After shaking at 150 rpm and 30 °C for 24 h in a thermostatic automatic shaker (HZQ-C, Haerbin, China), the adsorbents were separated from the solutions by filtration, and the filtrates were then titrated with a 0.1 M HCl or NaOH. The number of acidic groups was calculated based on the following assumptions: NaOH neutralizes carboxylic, lactonic, and phenolic groups; Na_2CO_3 neutralizes carboxylic and lactonic groups; and $NaHCO_3$ neutralizes only carboxylic groups. The number of basic sites was determined from the amount of HCl that reacted with the adsorbents.

2.3.3.2. DRIFTS. DRIFTS was performed in a Bruker Equinox 55 FTIR instrument with KBr Optics, an MCT detector, and ZnSe windows. The spectra were then collected at various intervals of time in Kubelka–Munck (K–M) mode without any manipulation. All the spectra were recorded at a resolution of 8 cm^{-1} with 200 scans.

2.3.3.3. TPD. TPD profiles were obtained using a tabular quartz microreactor of 6.0 mm in diameter and 370 mm in length inside an electric furnace, coupled with a quadrupolar mass spectrometer (Balzers QMG 422, Switzerland). About 30 mg samples of each adsorbent were heated in the reactor from room temperature to 1010 °C at a heating rate of 10 °C/min under a flow of Ar (99.99%, 40 mL/min). CO and CO_2 desorbed from the adsorbents were monitored by the mass spectrometer (MS) following the signals (*m*/*z*): 28 (CO) and 44 (CO_2).

2.4. Adsorption procedure

The adsorption experiments were carried out by adding about 0.500 g adsorbent into well-sealed glass flasks filled with 50 mL of adsorptive solution with different initial concentrations of phenol, aniline, and pyridine. The flasks were shaken at 150 rpm and 30 °C for 72 h to ensure equilibrium adsorption. The adsorbents were then separated from the solution by filtration and air-dried at room temperature. The equilibrium concentration of the filtrate was measured with a UV-vis spectrophotometer (Tech Comp UV2300, China) at 230, 252, and 270 nm wavelengths for aniline, pyridine and phenol, respectively. The amount of the aromatic compounds adsorbed on the adsorbents was determined from the difference in concentration of the adsorptive solutions before and after the adsorption. The equilibrium adsorption capacity (q_e) was defined as the amount of adsorbate per gram of adsorbent in mg/g and calculated by:

$$q_e = \frac{(C_i - C_e)V}{m}, \quad (1)$$

where C_i and C_e are the initial and equilibrium concentrations of an adsorptive solution (mg/L), respectively; V is the volume of the adsorptive solution (L); and m is the mass of the adsorbent (g).

3. Results and discussion

3.1. Characterization of the adsorbents

3.1.1. Chemical composition

Ash and elemental analyses of the three adsorbents are shown in Table 1. AC has an ash content of 8.32 wt.% and S of 0.46 wt.%; however, ash and S in ACF and ACFN have not been detected. Among the three adsorbents, AC has the lowest H, N, and O contents. Compared with ACF, ACFN has higher H, N, and O contents, indicating that HNO_3 oxidation chemically modified ACF, forming many H-, N-, and O-containing groups on the surface.

3.1.2. Texture

The textural parameters of the three adsorbents are presented in Table 2. As expected, the textural properties of ACF and ACFN are similar, indicating no major differences in the micro/mesopore range is caused by HNO_3 oxidation, as shown by the median pore width (Table 2) and the pore size distribution (Fig. 1). Both the mesopore properties (V_{meso} and S_{meso}) and the micropore volume

Table 1
Ash amount and elemental analysis of the adsorbents.

Adsorbent	Ash (wt.%)	C(wt.%)	H(wt.%)	S(wt.%)	N(wt.%)	O(wt.%)
AC	8.32	88.47	0.50	0.46	0.43	1.82
ACF	–	83.70	0.89	–	2.65	12.76
ACFN	–	70.40	1.59	–	2.89	25.12

Table 2
Textural properties of the adsorbents.

Adsorbent	V_{mic} (mL/g)	S_{meso} (m^2/g)	V_{meso} (mL/g)	$\bar{r}$ (nm)	S_{BET} (m^2/g)
AC	0.281	380	0.055	1.039	996
ACF	0.393	130	0.060	0.966	1004
ACFN	0.339	112	0.053	0.962	865

Note: $\bar{r}$ is the median pore width by Horvath–Kawazoe.

(V_{mic}) of ACFN slightly decreased. This is due to the presence of numerous oxygen-containing groups on the carbon surface, which may partially block the access of N_2 molecules into the micropores. In addition, the micropore volume of AC is much smaller than that of ACF and its mesopore surface area is even larger than that of ACF; however, the V_{meso} and S_{BET} of AC and ACF are similar. This indicates that AC, which is significantly different from ACF, has a very wide pore structure.

3.1.3. Characterization of surface chemistry

Table 3 shows the acid/base properties of the adsorbents characterized by Boehm titration. The surface acidic/basic groups in ACF are much higher than the corresponding parameters in AC, indicating the difference in surface chemistry between AC and ACF resulting from the different preparation of the carbon materials. Clearly, the HNO_3 oxidation increased the surface acidic groups (carboxylic, lactonic, and phenolic groups) and decreased the basic groups of ACF. Notably, some surface groups cannot be determined by Boehm titration, including anhydride and nitrogen-containing groups of adsorbents. DRIFTS and TPD of the three adsorbents were carried out in order to verify other groups on the surface of ACF.

The DRIFTS spectra of the adsorbents are shown in Fig. 2. As can be seen, among the three adsorbents, the lowest intensity of bands is in AC, indicating that AC has fewer groups than both ACF and ACFN. Compared with ACF, ACFN has stretching vibrations similar to those of ACF, with the exception of the stronger intensity of bands of the surface functionalities of ACFN with OH of around 3384 cm^{-1}, C=O (carboxylic, anhydride, lactone and ketene) at 1674 cm^{-1}, C–O (lactonic, ether, phenol, etc.) including υ_{as} (C–O) at 1300 cm^{-1}, and υ_s (C–O) at 1110 cm^{-1} [19]. This indicates that more oxygen-containing groups have been introduced on ACF surface after HNO_3 oxidation, which is in agreement with the data shown in Tables 1 and 3. Although the DRIFTS spectra do not provide quantitative information about the carbon surface chemistry, it can provide other results, such as nitrogen-containing groups, that could not be detected using the titration method due to their inability to dissociate. Clearly, ACFN has the strong band with the stretching vibrations around 1519 cm^{-1}, which can be ascribed to the presence of more nitro groups on the ACF surface [16].

The CO_2 and CO release curves of the adsorbents during TPD are shown in Fig. 3. Surface oxygen-containing groups on carbon materials decompose upon heating, releasing CO_2 and CO at different characteristic temperatures [22]. For example, the CO_2 released at temperatures lower than 400 °C may be ascribed to the decomposition of carboxylic acids, and at around 650 °C to the decomposition of lactones. CO_2 and CO released at temperatures around 550 °C account for the decomposition of anhydrides; the CO released at around 700 °C can be attributed to the decomposition of phenolic groups, and beyond 850 °C to the decomposition of carbonyl groups and quinones. Interestingly, as shown in Fig. 3, the HNO_3 oxidation resulted in increased amounts of carboxylic acids, lactones, anhydrides and phenolic groups, and less carbonyl groups and quinones on the surface. That the acidic groups increased the surface acid property of adsorbents concurs with the data shown in Table 3. Compared with AC, more CO_2 and CO evolved from ACF, indicating that the acid/base groups on the surface of ACF are plenty (Fig. 2, Tables 1 and 3).

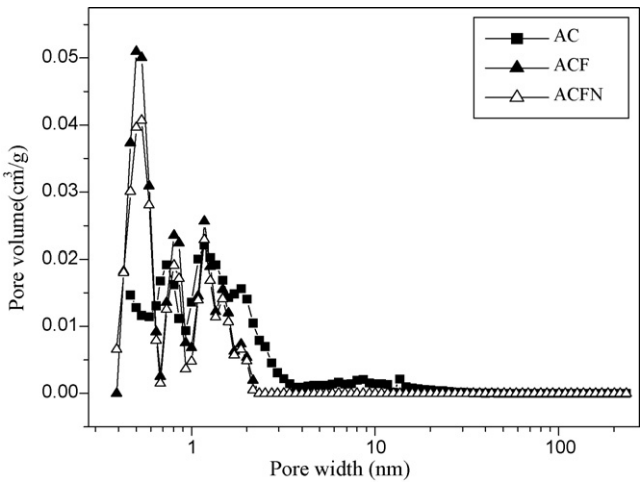

Fig. 1. Pore size distribution.

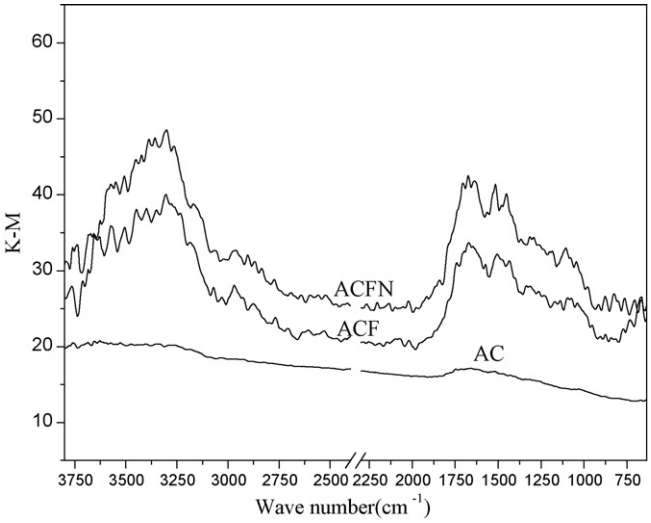

Fig. 2. DRIFTS spectra of the adsorbents.

Table 3
Surface chemistry of the adsorbents.

Adsorbent	Surface acidity (mmol/g)	Carboxylic (mmol/g)	Lactonic (mmol/g)	Phenolic (mmol/g)	Surface basicity (mmol/g)
AC	0.489	0.033	0.327	0.129	0.646
ACF	1.279	0.068	0.911	0.300	1.605
ACFN	3.724	1.409	1.224	1.091	1.383

Note: Surface acidity and surface basicity are the adsorbent's surface acidic groups and surface basic groups, respectively.

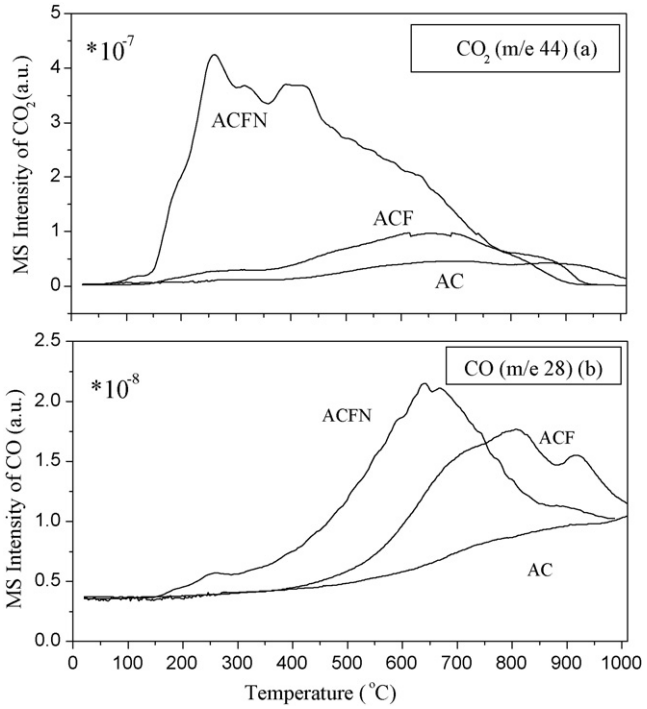

Fig. 3. TPD spectra of the 3 adsorbents: (a) CO_2 evolution and (b) CO evolution.

3.2. Adsorption studies

Selected properties of the adsorbates are shown in Table 4. The acid/base properties of the organic compounds are expressed as pK_a, which are 9.95 for phenol, 4.60 for aniline and 5.17 for pyridine. An aqueous solution of phenol is acidic, and those of aniline and pyridine are basic. The aqueous solubility of these compounds is significantly different, with an order of pyridine > phenol > aniline.

The Langmuir adsorption model has been frequently used to describe the adsorption behavior of aromatic compounds on AC [15,23]. This was chosen to fit the experimental adsorption data in this work. The model takes the form of:

$$q_e = q_m \frac{KC_e}{1 + KC_e}, \quad (2)$$

where q_e (mg/g) is the amount of an aromatic compound adsorbed on an adsorbent at an equilibrium concentration C_e (mg/L); q_m (mg/g) is the Langmuir parameter representing the maximum adsorption capacity of the aromatic compound on the adsorbent; and K (L/mg) is the Langmuir parameter related to the heat of adsorption.

Table 4
Selected properties of the adsorbates.

Solute	Phenol	Aniline	Pyridine
Aqueous solubility (25 °C, g/kg)	67	34	∞
pK_a	9.95	4.60	5.17
pH	<7	>7	>7

Fig. 4 depicts the adsorption isotherm of aniline, phenol, and pyridine on the different adsorbents at 30 °C. The experimental data are represented as symbols and the Langmuir model as solid lines. Clearly the Langmuir model can well describe the experimental data. The Langmuir parameters (q_m and K) for aniline, phenol, and pyridine, as determined through the fitting, are given in Table 5.

Obviously, for the same equilibrium concentration of each aromatic compound, the equilibrium adsorption capacity of AC is always less than that of ACF, which is caused mainly by the lower micropore volume of AC (Table 2 and Fig. 1). The mechanism for adsorption should be that adsorption sites of adsorbents for aromatic compounds increase with increase in micropore volume.

As shown in Fig. 4, the adsorption behaviors of ACFN and ACF are different for the same aromatics. For the same equilibrium concentration, the adsorption amount of the same compounds obviously increased for ACFN < ACF, similar to the trend of q_m. It indicates that HNO_3 oxidation significantly reduced the ability of ACF to adsorb compounds. Due to the similar structural properties of ACF and ACFN, the difference in amount of each aromatic compound adsorbed on ACFN and ACF can be attributed only to the effect of surface chemistry (mainly oxygen-containing groups). It can thus be concluded that the oxygenated groups on the surface of ACF play an important role in the adsorption of the aromatic compounds.

In the interaction of liquid aromatic compounds with activated carbons, there are principally dispersive interaction, electrostatic interaction, and water cluster blocking [8]. In this study, adsorptive solutions were all unadjusted. As implied by the pK_a of the organic compounds and the pH of the adsorptive solutions (Table 4), aniline, phenol, and pyridine are all predominantly in the molecular form in solution, which accords with dispersive interaction. Dispersive interaction is thus expected to play a significant role in the adsorption process of each compound. The dispersive interaction refers to the interaction of the π orbit on the carbon basal planes with the electron density of the aromatic rings. The dispersive interaction is easily influenced by π electron density in the basal plane of adsorbents. Due to their deactivating role, surface oxygen-containing groups reduce π electron density in the basal planes of the adsorbents; this weakens the π–π dispersive interaction and consequently lowers the adsorption capacity [24].

Due to the complexity of liquid phase adsorption (aromatic compounds and water coexist in an adsorptive solution), the effects of water (as a solvent) [25–28] on the adsorption capacity of aromatic compounds should also be taken into account. Aromatic compounds (aromatic ring is non-polar) adsorb mainly

Table 5
Langmuir parameters obtained through linear regression of the data in Fig. 4.

Adsorbent	Solute	q_m (mg/g)	K (L/mg)
AC	Aniline	241.5	0.0158
ACF		271.7	0.0693
ACFN		244.2	0.0391
AC	Phenol	211.1	0.0426
ACF		241.4	0.0495
ACFN		164.8	0.00606
AC	Pyridine	150.8	0.00776
ACF		175.3	0.00702
ACFN		145.8	0.00895

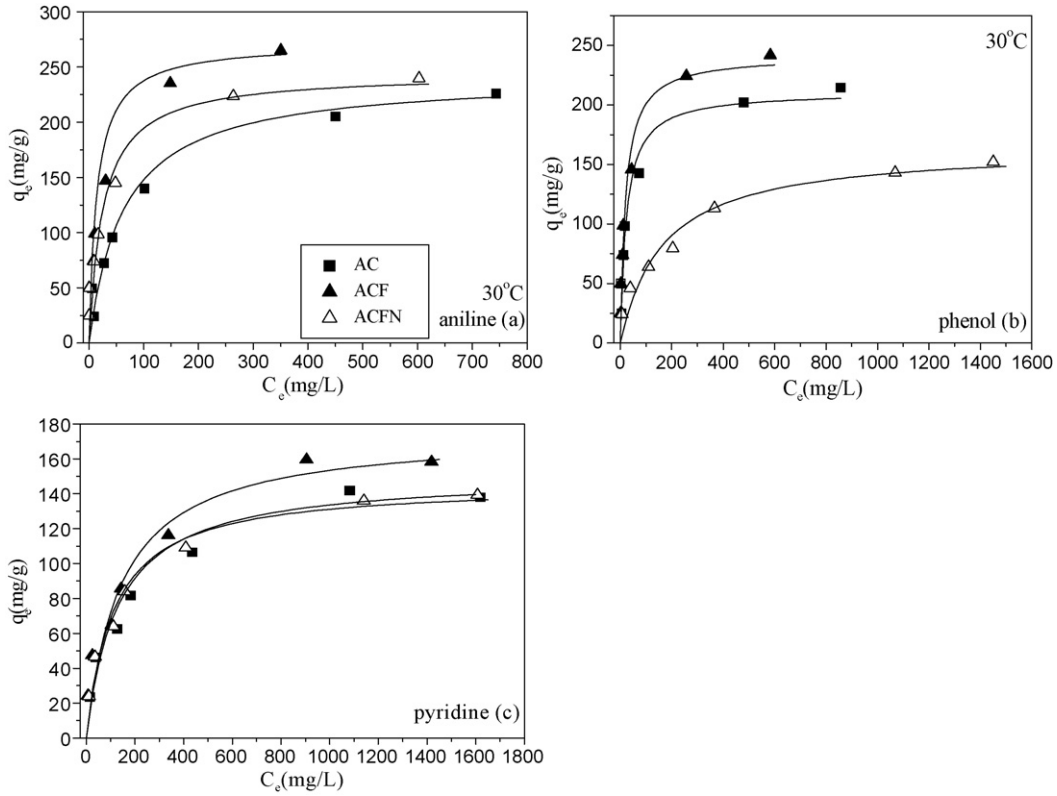

Fig. 4. Adsorption isotherms of aromatics on adsorbents at 30 °C.

onto hydrophobic surfaces and water adsorbs onto polar surfaces because both water and oxygenated groups are polar, which may be competitively adsorbed onto the non-polar and polar surfaces, respectively. In a previous study [29], water adsorption is promoted by acidic oxygen-containing groups on the surface of the adsorbents. In this experiment, the HNO_3 oxidation increased the surface acidic groups on ACF, which may enhance the hydrophilic property of the ACF and finally increase its water adsorption capacity. Its mechanism is probably related to the H-bonds formed between the water molecules and the surface oxygen-containing groups (e.g., carboxylic acid) [28,30], making water easier to adsorb onto oxygenated sites than aromatics. The adsorbed water may form more water clusters in a 3D configuration, which may block the pores through which aromatic molecules cannot pass into micropores [22,30].

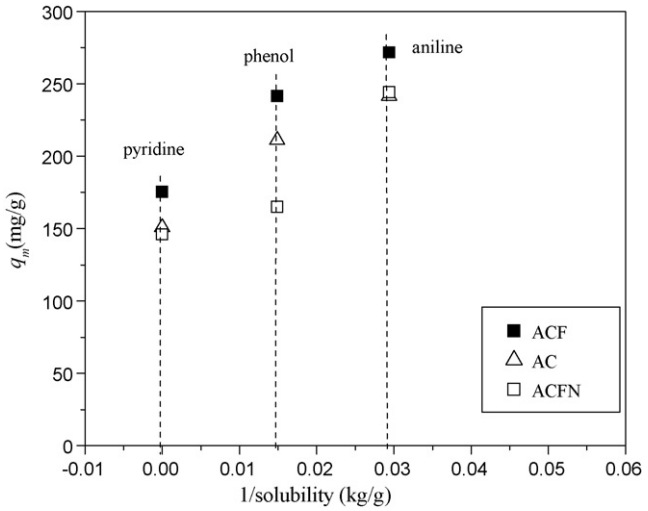

Fig. 5. Relationship between q_m and solubility of the compounds.

Notably, the maximum adsorption capacity (q_m) of the aromatic compounds on the same adsorbent is significantly different (Table 5), in the order of aniline > phenol > pyridine. Fig. 5 shows the relationship between q_m and the solubility of the aromatic compounds (represented as 1/solubility to avoid infinite solubility of pyridine in water). A decrease in solubility (or an increase in 1/solubility) corresponds to an increase in q_m for the same adsorbent, which concurs with data reported for nitrobenzene > aniline > phenol in literature [8]. This difference in q_m, although influenced by many factors, can be attributed mainly to the difference in the solubility of the adsorbate in water.

In the Langmuir adsorption model, K is also an important parameter; therefore, the correlation between K and surface chemistry of the adsorbents (figure is not shown) was investigated. The K of aniline, phenol, and pyridine can be indirectly associated with the surface chemistry of adsorbents, indicating that K may be influenced by other factors in adsorbing the aromatic compounds. Due to the complexity of liquid phase adsorption, these factors will be investigated in future studies.

4. Conclusion

ACF oxidized by HNO_3 has a similar texture to originals; however, the surface acidic groups (mainly oxygen-containing groups such as carboxylic acids, phenolic groups, lactones, and anhydrides) are significantly increased.

The surface acidic groups of ACF play an important role in the adsorption of aromatics. The increase of the surface acidic groups of ACFs significantly reduced the adsorption capacity of ACF for aromatics because the π–π dispersive interaction between ACF and aromatic compounds decreased, competition of water adsorption increased because of increase of hydrophilic property of ACF, and

more water clusters formed to block the entry of the compounds into micropores. In addition, the *K* of aniline, phenol, and pyridine is found to be indirectly related with the surface chemistry of ACF.

Furthermore, the micropore volume in activated carbon materials demonstrated an active influence on aromatic compound adsorption. For the same aromatic compound, the adsorption capacity of activated carbon materials increases with increase in their micropore volume. The aqueous solubility of aromatic compounds, such as aniline, pyridine and phenol, has an important effect on the adsorption capacity of activated carbon materials. The maximum adsorption capacity of the same adsorbent for aniline, pyridine, and phenol increases with the decrease in the aqueous solubility of adsorbates.

The results stated above indicate that activated carbon materials with higher micropore volume and lower surface acidic groups can be optimized for the adsorption of aromatic compounds in water.

Acknowledgements

The authors express their grateful appreciation for the financial support from the Doctorate Science Fund of Taiyuan University of Science & Technology (20102001) and the Shanxi Province Basic Research Project (2008011014-3).

References

[1] H. Hindarso, S. Ismadji, F. Wicaksana, Mudjijati, N. Indraswati, J. Chem. Eng. Data 46 (2001) 788.
[2] X. Xie, L. Gao, J. Sun, Colloids Surf. A 308 (2007) 54.
[3] W. Cai, J. Li, Z. Zhang, J. Hazard. Mater. 148 (2007) 38.
[4] A. Cybulski, J. Trawczyński, Appl. Catal. B: Environ. 47 (2004) 1.
[5] C.H. Ko, C. Fan, P.N. Chiang, M.K. Wang, K.C. Lin, J. Hazard. Mater. 149 (2007) 275.
[6] A.A. Gürten, S. Uçan, M.A. Zler, A. Ayar, J. Hazard. Mater. 120 (2005) 81.
[7] M. Yu, J.T. Hunter, J.L. Falconer, R.D. Noble, Microporous Mesoporous Mater. 96 (2006) 376.
[8] F.P. Villacańas, M.F.R. José, J.M. Órfão, J.L. Figueiredo, J. Colloid Interface Sci. 293 (2006) 128.
[9] Y. Matatov-Meytal, O. Nekhamkina, M. Sheintuch, Chem. Eng. Sci. 54 (1999) 1505.
[10] Z. Lei, Z. Liu, Fuel Process. Technol. 88 (2007) 607.
[11] Y.I. Matatov-Meytal, M. Sheintuch, Ind. Eng. Chem. Res. 36 (1997) 4374.
[12] H. Greene, D. Prakash, K. Athota, G. Atwood, C. Vogel, Catal. Today 27 (1996) 289.
[13] J. Zhao, Z. Liu, D. Sun, J. Catal. 227 (2004) 297.
[14] K. László, Colloids Surf. A 265 (2005) 32.
[15] N. Wibowo, L. Setyadhi, D. Wibowo, J. Setiawan, S. Ismadji, J. Hazard. Mater. 146 (2007) 237.
[16] I.I. Salame, T.J. Bandosz, J. Colloid Interface Sci. 240 (2001) 252.
[17] H.P. Boehm, Carbon 40 (2002) 145.
[18] E. Ayranci, O. Duman, J. Hazard. Mater. 136 (2006) 542.
[19] V.M. Gun'ko, V.V. Turov, O.P. Kozynchenko, D. Palijczuk, R. Szmigielski, S.V. Kerus, M.V. Borysenko, E.M. Pakhlov, P.P. Gorbik, Appl. Surf. Sci. 254 (2008) 3220.
[20] M.F.R. Pereira, S.F. Soares, J.J.M. Órfão, J.L. Figueiredo, Carbon 41 (2003) 811.
[21] J.J.M. Órfão, A.I.M. Silva, J.C.V. Pereira, S.A. Barata, I.M. Fonseca, P.C.C. Faria, M.F.R. Pereira, J. Colloid Interface Sci. 296 (2006) 480.
[22] O.P. Mahajan, C. Moreno-Castilla, P.L. Walker, Sep. Sci. Technol. 15 (1980) 1733.
[23] P.C.C. Faria, J.J.M. Órfão, M.F.R. Pereira, Water Res. 38 (2004) 2043.
[24] R.W. Coughlin, F.S. Ezra, Environ. Sci. Technol. 2 (1968) 291.
[25] H.A. Arafat, M. Franz, N.G. Pinto, Langmuir 15 (1999) 5997.
[26] W.H. Lee, P.J. Reucroft, Carbon 37 (1999) 7.
[27] E.A. Müller, K.E. Gubbins, Carbon 36 (1998) 1433.
[28] M. Franz, H.A. Arafat, N.G. Pinto, Carbon 38 (2000) 1807.
[29] B. Li, Z. Lei, Z. Huang, Chem. Eng. Technol. 32 (2009) 763.
[30] A. Dąbrowski, P. Podkościelny, Z. Hubicki, M. Barczak, Chemosphere 58 (2005) 1049.